Millimeter and Submillimeter Wave Quasi-Optical Oscillator with Multi-Elements

Millimeter and Submillimeter Wave Quasi-Optical Oscillator with Multi-Elements

Hirotaka Kondo, Masashige Hieda, Masatoshi Nakayama, Toshihide Tanaka, Katsumi Osakabe, and Koji Mizuno, *Senior Member, IEEE*

Abstract—Multi-element oscillators with a quasi-optical resonator are reported. The resonator consists of a Fabry–Perot cavity with a grooved mirror (grating) and a concave mirror. It is possible to mount solid-state devices (Gunn diode, GaAsMESFET, etc.) in the grooved mirror. The oscillator has capability for power-combining of solid-state sources in the millimeter and submillimeter wave regions.

I. INTRODUCTION

RECENTLY, many kinds of oscillators have been developed in the millimeter and submillimeter wave regions (electron tube, gas laser, solid-state device). Solid-state devices have many advantages: small size, light weight, and low-voltage power supplies. As frequency increases, however, output power becomes small, and frequency stability and noise characteristics also become a problem. Power-combining of multi-elements is effective as to the former. High-Q resonator and power-combining are effective as to the latter. Therefore, coherent power-combining of a large number of devices using quasi-optical resonators is attractive [2], [3]. We have been investigating a quasi-optical Fabry–Perot cavity with a grooved mirror and a concave mirror. We have used this cavity in an electron tube called the Ledatron [1]. In the Ledatron, a ribbon-like electron beam interacts with distributed electric field along the grating surface. We have also studied the same configuration with solid-state devices (Fig. 1) in stead of the electron beam because of the above advantages of the devices.

Using this structure, coherent power-combining and frequency-locking of 18 Gunn diodes (6 × 3) and 6 GaAsMESFET's (3 × 2) have been successfully observed at the X-band [4], [5].

This paper describes about mainly our U-band (50 GHz) Gunn diode oscillators. In the next section, the configuration of the oscillator is shown, and a simple equivalent circuit is given. Experimental characteristics of the U-band oscillator are presented in Section III. A quasi-optical method as an output coupler is also studied. In Section IV is described our W-band Gunn oscillator. In Section V, a AFC (Automatic Frequency Control) method using a commercially available FM-detector has success-
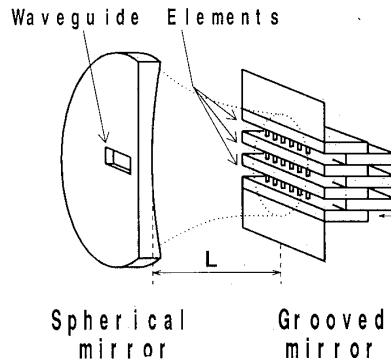
Fig. 1. The resonator configuration.

fully been used in the frequency stabilization for X-band and U-band oscillators. Section VI is for summary and conclusion.

II. CONFIGURATION AND EQUIVALENT CIRCUIT

The configuration of our resonator is shown in Fig. 1. It consists of a grooved mirror (grating) and a concave mirror facing each other. The concave mirror's radius of curvature and the mirrors' size have been determined for the following factors: (i) resonant mode spot size (radius) on the grating should be equal to a half the area on which the diodes are mounted (the spot size diameter equals to the diodes-area), (ii) the semiconfocal configration is adapted to obtain the minimum diffraction loss for the fundamental TEM_{00} mode. The spot sizes on the grating and the concave mirror can be calculated theoretically. The spot size on the grooved mirror is given by

$$\omega_0^4 = \left(\frac{\lambda}{\pi}\right)^2 \frac{L(R_1 - L)(R_2 - L)(R_1 + R_2 - L)}{(R_1 + R_2 - 2L)^2}$$
$$\rightarrow \left(\frac{\lambda}{\pi}\right)^2 L(R_1 - L) \quad (R_2 \rightarrow \infty), \qquad (1)$$

where L is the resonator length (see Fig. 1), λ the wavelength, R_1, R_2 the concave and the grooved mirrors' radius of curvature, respectively ($R_1 = 100$ mm for our U-band oscillator, $R_2 = \infty$). The spot size on the concave mirror is

$$\omega_1^2(L) = \omega_0^2 \left[1 + \left(\frac{\lambda L}{\pi \omega_0^2}\right)^2\right]. \qquad (2)$$
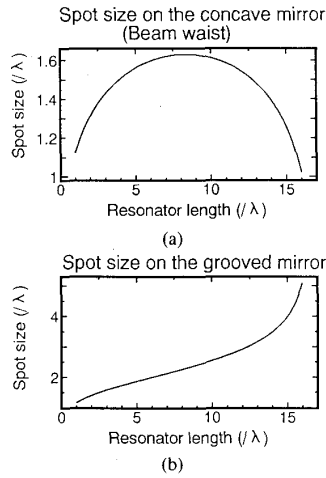
Fig. 2. Calculated sizes on the mirrors versus the resonator length. (a) The spot size (beam waist) on the grating. (b) The spot size on the concave mirror. (f = 50 GHz, concave mirror's radius of curvature = 100 mm).

Fig. 2 shows how the spot sizes on both the mirrors vary with the resonator length L. The groove pitch D must be less than the wavelength to avoid diffraction loss.

The Gunn diodes are mounted in grooves and biased by the top and the bottom plates of each groove (Fig. 3). These plates are insulated by thin (80 μm) teflon tape. The groove depth t can be continuously changed to adjust the impedance of the groove. Output power is taken out by a waveguide at the center of the concave mirror. Quarter-wavelength choke structures are cut on the plates. A quasi-optical output coupler can also be adopted, which will be mentioned in Section IV.

The spacing between the adjacent diodes in a groove is n (odd-integer) multiplied by a half the wavelength so that a guided wave in the groove can not be excited while the TEM_{00} mode in the resonator is excited. Considering the diode case dimension ($\sim \lambda/2$) the minimum integer n is 3 for our 50 GHz oscillator. For a 3 × 3 diode array, the diode area is $3\lambda \times (4/3)\lambda$, since the groove pitch is chosen to $(2/3)\lambda$. Since the spot size diameter on the grating equals the diodes-area, the grating dimention should be larger than two times the diodes-area in order to avoid the diffraction loss. The total cavity size is determined using Fig. 2, leading to about $(10\lambda)^3 \sim (15\lambda)^3$.

The resonator proposed here has the following advantages: it has a large heat dissipation capacity, can mount large number of devices, is large enough than the wavelength, and has simple bias circuit.

A. Resonant Frequency

The resonant frequency of a Fabry–Perot cavity with a concave mirror and a plane mirror is given by

$$f = \frac{c}{2L}\left[q + \frac{(m + n + 1)}{\pi} \arctan\left(\frac{L}{R_1 - L}\right)^{1/2}\right], \quad (3)$$

where c is the light velocity, L the resonator length, q the number of longitudinal mode, m and n the number of

$$D = 0.67\lambda \quad d = 0.17\lambda$$
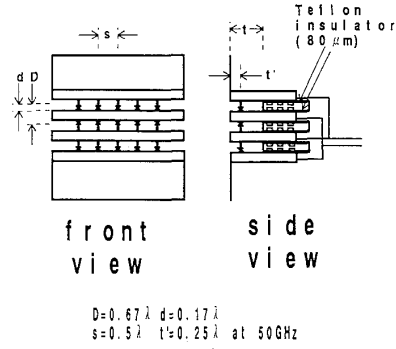$$s = 0.5\lambda \quad t' = 0.25\lambda \quad \text{at 50GHz}$$

Fig. 3. The grooved mirror for mounting diodes.

transverse mode (TEM_{mn}), R_1 the concave mirror's radius of curvature. Since in our cavity configuration, a grooved mirror is used instead of a plane mirror, the resonant frequency is given by

$$f = \frac{c}{2L}\left[q + \frac{(m + n + 1)}{\pi} \arctan\left(\frac{L}{R_1 - L}\right)^{1/2} + \frac{\theta}{2\pi} - \frac{1}{2}\right], \quad (4)$$

where $\exp(j\theta)$ is a reflection coefficient of the grooved mirror. We have calculated the reflection coefficient of the grating by the following method [1]. For simplicity, we assume that (i) grating is infinite in two-dimension, (ii) a plane wave enters perpendicularly to a surface of the grating (Fig. 4). Under these condition, we can consider this structure as a plane parallel line with a pitch of D. We get the electric and magnetic field expression for Region (I) as follows:

$$E_y^I(y, z) = -2j \sin(\beta_0 z) + \sum_{n=0}^{\infty} A_{2n} \cos\left(\frac{2n\pi}{D} y\right) e^{j\beta_{2n}z}, \quad (5)$$

$$H_x^I(x, y) = -\frac{2\omega\epsilon}{\beta_0} \cos(\beta_0 z) + \sum_{n=0}^{\infty} A_{2n} \cdot \cos\left(\frac{2n\pi}{D} y\right) e^{j\beta_{2n}z}, \quad (6)$$

where

$$\beta_{2n} = -j\sqrt{(2n\pi/D)^2 - (2\pi/\lambda)^2}. \quad (7)$$

In Region (II), the fields are similarly given by

$$E_y^{II}(y, z) = \sum_{s=0}^{\infty} B_{2s} \cos\left(\frac{2s\pi}{d} y\right) \frac{\sin[\zeta_{2s}(z - t)]}{-\sin(\zeta_{2s}t)}, \quad (8)$$

$$H_x^{II}(x, y) = \sum_{s=0}^{\infty} j\omega\epsilon B_{2s} \cos\left(\frac{2s\pi}{d} y\right) \frac{\cos[\zeta_{2s}(z - t)]}{\sin(\zeta_{2s}t)}, \quad (9)$$

where

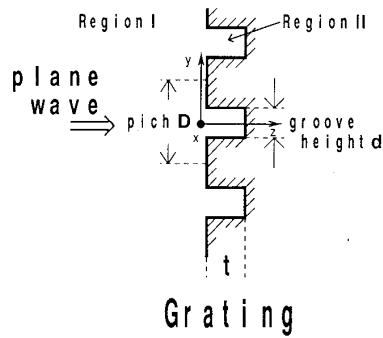$$\zeta_{2s} = -j\sqrt{(2s\pi/d)^2 - (2\pi/\lambda)^2}. \quad (10)$$

Fig. 4. Grooved mirror structure showing notations for calculation a reflection coefficient.

For fulfilling the boundary conditions at $z = 0$ (grating surface), the undetermined coefficients A_{2n} and B_{2s} are decided and the refrection coefficient at the grating is given by

$$\Gamma = e^{j\theta} = A_0 - 1. \tag{11}$$

Fig. 5 compares the calculated resonant frequencies using (4) and (11) with measured results (at 50 GHz), showing a good agreement between them.

A fringing capacitance across a groove edge can also be given using this calculation, and will be used in a cavity equivalent circuit described later.

B. Q-Value

We have measured Q-value of a 10 GHz model resonator with a grooved mirror. Fig. 6 shows experimentally obtained Q-values as a function of the groove depth. There is a minimum for the Q-value at the groove depth of about 0.24 wavelength which corresponds to the anti-resonant state of the groove. In this state, the electric field inside the groove becomes large, leading to increase of ohmic loss. Consequently in our cavity configuration the groove depth is set to about a wavelength and the diode position is about a quarter the wavelength from the bottom of the groove in order to obtain the impedance matching between the diode and the circuit. The Q-value of our 50 GHz cavity was measured by a network analyzer (HP 8510B), and is about 300. This low value is due to large coupling by a waveguide (WR-19) at the center of the concave mirror, since we are, at the moment, interested in power rather than monochromaticity.

C. Equivalent Circuit

Fig. 7 shows an equivalent circuit of our oscillator. Considering the periodicity of the configuration (Section II), Region(I) and Region(II) (Fig. 4) can be expressed by a plane parallel line with a characteristic impedance of Z_1 = 377 Ω and $Z_2 = (d/D) \times 377$ Ω, respectively. The fringing capacitance is calculated according to the analysis in Section II. The impedance of the post under which the diode is set can be also calculated theoretically [6]. Z_l represents output coupling, and was calculated by the re-
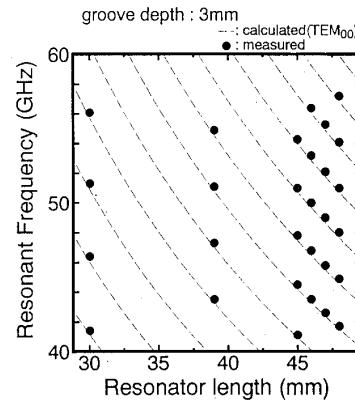

Fig. 5. Comparison between the calculated and measured resonant frequency of a Fabry–Perot resonator with a grooved mirror ($f = 50$ GHz).
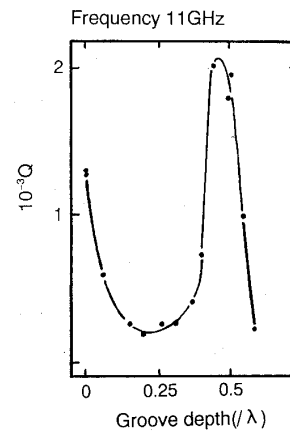

Fig. 6. Measured Q-value of the resonator with a grooved mirror as a function of the groove depth ($f = 11$ GHz).
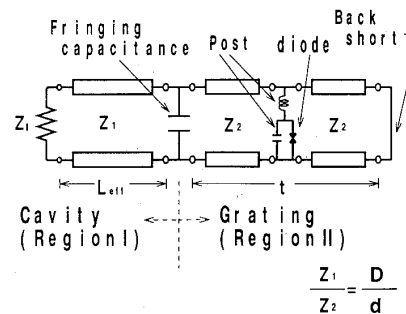

Fig. 7. The equivalent circuit of our oscillator.

flection coefficient of the mirror, which was approximately given by considering the area ratio of the spot size there and the output waveguide. Since the wavelength in the resonator is different from that in the free space, the resonator length L_{eff} is given by the following equation:

$$L_{eff} = L - \frac{\arctan\left(\dfrac{L}{R_1 - L}\right)^{1/2}}{\beta}, \tag{12}$$

where $\beta(= 2\pi/\lambda_0)$ is the propagation constant in vacuum [7]. This equivalent circuit of Fig. 7 is used to calculate oscillation frequency, the optimum position of the diode, and so on.

III. U-BAND GUNN DIODE OSCILLATOR

A. Spectrum and Tuning Range

Fig. 8(a) and (b) show the spectra of our U-band oscillators with a single diode and 3 diodes, respectively. The grating configuration was described in Section II. The groove height is $\lambda/6$ (1 mm at 50 GHz) for both the oscillators.

With 3 diodes oscillator, we have obtained about 50% larger than the power from a single diode. The reason that the output is not three times is that we have not optimized the output coupling. The Carrier-Noise ratio is improved about 4.8 dB as expected theoretically [8].

Fig. 9 shows how the oscillation frequency varies with the resonator length L for 3 Gunn diodes oscillator. The broken line shows the resonant frequency calculated by the equivalent circuit described in Section III. The measurement agrees with the calculation. The mechanical tuning range is about 1.8 GHz (3.2%).

B. Oscillator with a Fabry–Perot Coupler

In the millimeter and submillimeter wave regions, quasi-optical coupling is effective for many cases. Fig. 10 shows an oscillator with a Fabry–Perot coupler with two half-transmission mirrors in place of the concave mirror in Fig. 1. The half-mirrors are made of copper-clad substrates with a thin polyimide of 50 μm thickness etched by making use of photo-lithography. The mesh period is 2.4 mm, the width of the copper line is 0.4 mm, and the transmission is -5 dB at 50 GHz.

We have measured output radiation pattern in front of the Fabry–Perot coupler using a small horn antenna. Fig. 11 shows the output beam pattern measured by scanning the horn antenna vertically against the axis of the resonator. It can be seen that the pattern is nealy the fundamental Gaussian mode (solid line).

IV. W-BAND GUNN DIODE OSCILLATOR

We have constructed a W-band oscillator with the same resonator configuration with a InP Gunn diode (Acrotec NT-W50). Fig. 12 shows how oscillation frequency varies with the resonator length L. The InP Gunn diode is mounted at the center of the grating. The mechanical tuning range is 1.8 GHz (2.3%). So far the maximum output power is 5.7 dBm. We are optimizing coupling and groove impedance to extract more power.

V. FREQUENCY STABILIZATION WITH AFC

A. AFC Stabilization

We have demonstrated oscillation frequency stabilization of our oscillators using a AFC (automatic frequency control) method. Our AFC circuit consists of a commer-
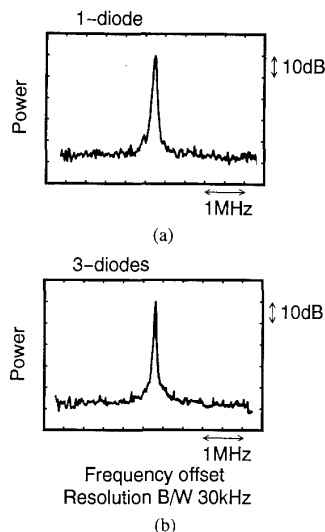

Fig. 8. Output spectra of U-band oscillators. (a) Single diode ($L = 85.4$ mm, $f_c = 53.8$ GHz). (b) 3 diodes ($L = 87.6$ mm, $f_c = 55.8$ GHz).
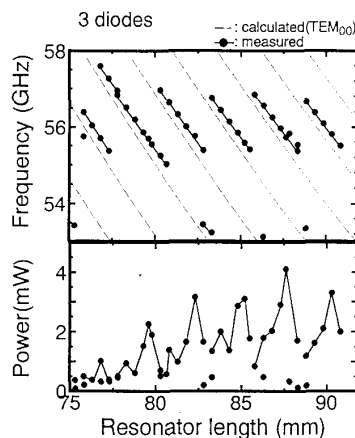

Fig. 9. Oscillation frequency and output power of the U-band oscillator with 3 Gunn diodes versus resonator length (groove depth = 5.44 mm). Broken lines show theoretical resonance frequencies of the TEM_{00} mode.
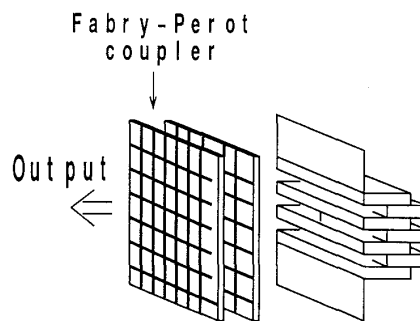

Fig. 10. Configuration of the Fabry–Perot output coupler.

cially available frequency discriminator for a broadcasting FM-receiver (NEC μPC1028H). Fig. 13 is the block diagram of the circuit. Using a waveguide mixer, an IF signal (10.7 MHz) is obtained by harmonic-mixing a part
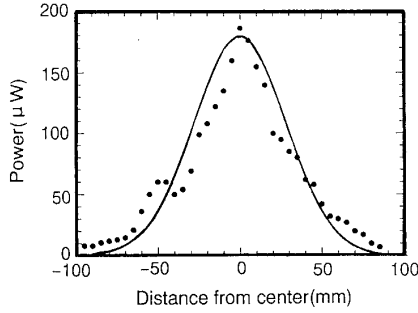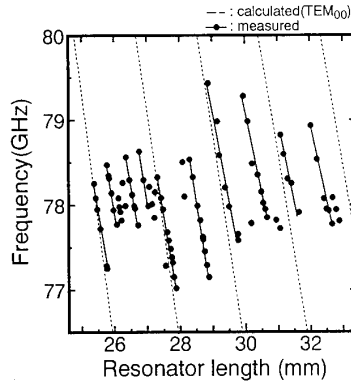
Fig. 11. Output beam pattern in front of the Fabry–Perot coupler.

Fig. 13. Block diagram of the AFC circuit.

Fig. 12. Oscillation frequency of a *W*-band Gunn diode oscillator versus resonator length (groove depth = 5.51 mm). Broken lines show theoretical resonance frequencies of the TEM_{00} mode.
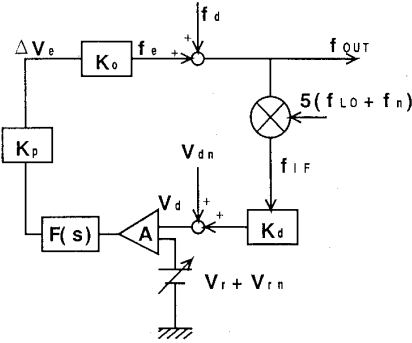
Fig. 14. Block diagram showing the deviations in the AFC circuit.

of the output power with a stabilized local power. The IF signal is converted to dc signal at the discriminator and the dc signal is compared with a standard voltage of a Zener diode. The difference (error) signal is fed back into a varactor mounted in a groove of the grating. Fig. 14 is a block diagram showing deviations, taking into consideration about noises in this circuit. From Fig. 14, we obtain the following relations:

$$f_{\text{IF}} = f_{\text{OUT}} - 5(f_{\text{LO}} + f_n),$$

$$V_d = K_d f_{\text{IF}} + V_{dn},$$

$$\Delta V_e = K_p F(s) A\{(V_r + V_{rn}) - V_d\},$$

$$f_e = K_0 \Delta V_e,$$

$$f_{\text{OUT}} = f_e + f_d,$$

thus, for $K_0 K_d A K_p F(s) \gg 1$, one has

$$f_{\text{OUT}} = \frac{f_d}{K_0 K_d K_p A F(s)} + \frac{(V_r + V_{rn}) - V_{dn}}{K_d}$$
$$+ 5(f_{\text{LO}} + f_n), \tag{14}$$

where K_p is a gain of the power supply, K_d conversion coefficient of the frequency discriminator (frequency sen-

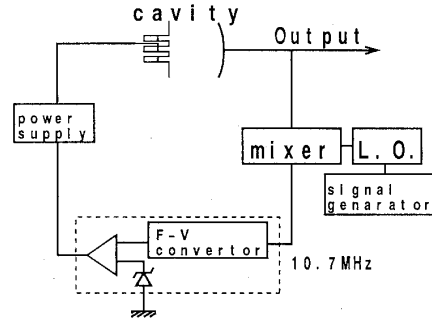sitivity), K_0 conversion coefficient of the oscillator (voltage sensitivity), $F(s)$ transfer function of the loopfilter (Laplace representation), f_d frequency drift of the oscillator, f_n frequency drift of the local oscillator, V_{dn} additional noise in the frequency discriminator, V_{rn} voltage drift of the Zener diode. It can be seen that the frequency drift f_d is improved in proportion to the open-loop-gain $(A K_0 K_d K_p F(s))$, and the noises (V_{dn}, V_{rn}) in the frequency discriminator and the Zener diode are improved in proportion to the frequency sensitivity (K_d). However, the drift of the local oscillation f_n remains. The local oscillator (*X*-band) is stabilized with a crystal oscillator at the 100 MHz region (HP synthesizer Model 8657A).

A. Stabilization of U-band Oscillator

We have applied this AFC method for our *U*-band oscillator with a single Gunn diode. The Gunn diode was

$$f_{\text{OUT}} = \frac{f_d + A K_0 K_p F(s) \{(V_r + V_{rn}) - V_{dn}\} + 5 K_0 K_d A F(s) K_p (f_{\text{LO}} + f_n)}{1 + K_0 K_d A F(s) K_p}, \tag{13}$$

mounted in the center groove, and in anther groove was set a varactor diode into which the error signal was fed. Fig. 15 shows the spectra without AFC (a) and with AFC (b). It can be seen that with AFC the C-N ratio was improved about 10 dB at a 100 kHz offset. The frequency stability (= frequency drift/oscillation frequency) was explained by the analysis described above.
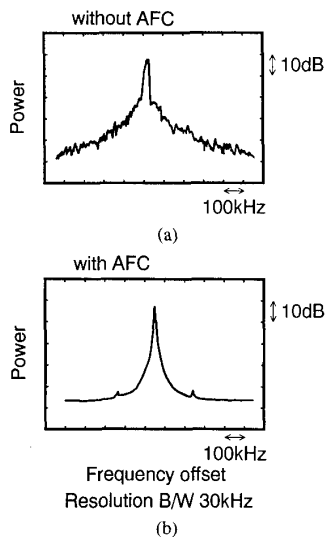
without AFC

(a)

with AFC

100kHz

Frequency offset

Resolution B/W 30kHz

(b)

Fig. 15. Spectra of the U-band oscillator, with a single Gunn diode and a varactor diode. (a) Without AFC (f_c = 56.131 GHz). (b) With AFC (f_c = 56.200000 GHz).
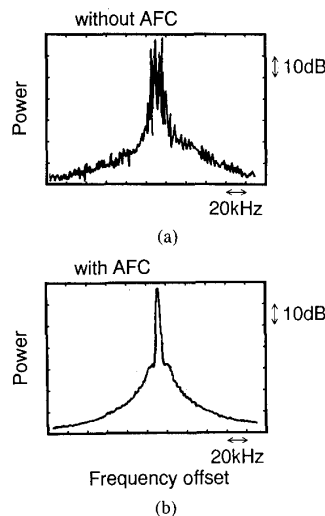
without AFC

20kHz

(a)

with AFC

20kHz

Frequency offset

(b)

Fig. 16. Spectra of the X-band oscillator, with 3 Gunn diode. (a) Without AFC (f_c = 11.031 GHz). (b) With AFC (f_c = 11.003786 GHz).

B. Stabilization of X-band Osillator

We have also demonstrated the usefulness of the AFC circuit for our X-band oscillator with 3 Gunn diodes. The error signal was fed back into a bias voltage of one of the diodes. Fig. 16 shows the spectra without AFC (a) and with AFC (b). It can be seen that all the three diodes were locked with the stabilized diode.

VI. CONCLUSION

We have demonstrated the utility of a quasi-optical resonator with multi-elements as a millimeter wave oscillator. The resonator consists of a Fabry–Perot cavity with a grooved mirror and a concave mirror. It has the capa-

bility of power combining of many solid-state sources at the millimeter and, possibly the submillimeter wave regions. Frequency-locking and coherent power combining of 3 Gunn diodes have been successfully observed at U-band. We have also reported a W-band Gunn diode oscillator with the same configuration. Frequency stabilization using a simple circuit (AFC) has been performed for a U-band (single diode) and a X-band (3 diodes) oscillators.

REFERENCES

[1] K. Mizuno and S. Ono, "The ledatron," in *Infrared and Millimeter Waves*, vol. 1, K. Button, Ed. New York: Academic Press, 1979, ch. 5.
[2] D. B. Rutledge, Z. B. Popović, R. M. Weikle II, M. Kim, K. A. Potter, R. C. Compton, and R. A. York, "Quasi-optical power-combining arrays," in *1990 IEEE MTT-S Int. Microwave Symp. Dig.*, pp. 1201–1204.
[3] K. D. Stephan and T. Itoh, "Recent efforts on planar components for active quasi-optical applications," in *1990 IEEE MTT-S Int. Microwave Symp. Dig.*, pp. 1205–1208.
[4] K. Mizuno, T. Ajikata, M. Hieda, and M. Nakayama, "Quasi-optical resonator for millimeter and submillimeter wave solid-state sources," *Electron. Lett.*, vol. 24, pp. 792–793, June 1988.
[5] M. Nakayama, M. Hieda, T. Tanaka, and K. Mizuno, "Quasi-optical resonator for millimeter and submillimeter wave solid-state sources," in *1990 IEEE MTT-S Int. Microwave Symp. Dig.*, pp. 1209–1212.
[6] R. L. Eisenhart, and P. J. Khan, "Theoretical and experimental analysis of a waveguide mounting structure," *IEEE Trans. Microwave Theory Tech.*, vol. MTT-19, no. 8, pp. 706–719, Aug. 1971.
[7] A. Yariv, *Introduction to Optical Electronics*. New York: Holt, Rinehart and Winston, 1971.
[8] T. Makino, M. Nakajima, and J. Ikenoue, "Noise reduction mechanism of a power combining oscillator system," *Trans. Institute of Electronics, Information and Communication Engineers*, vol. J62-B, no. 4, pp. 345–351, Apr. 1979 (in Japanese).

Hirotaka Kondo was born in Aichi, Japan, on May 26, 1966. He received the B.E. degree in electronic engineering from Tohoku University, Sendai, Japan in 1990. He is currently working for the M.E. degree in the field of millimeter- and submillimeter-wave quasi-optical oscillator with Multi-elements at Research Institute of Electrical Communication of Tohoku University.

Mr. Kondo is a member of the Institute of Electronics, Information and Communication Engineers of Japan.

Masashige Hieda was born in Toyama, Japan, on August 6, 1965. He received the B.E. and M.E. degrees in electronic engineering from Tohoku University, Sendai, Japan, in 1988 and 1990, respectively.

In 1990 he joined Mitsubishi Electric Corporation, Kanagawa, Japan.

Mr. Hieda is a member of the Institute of Electronics, Information and Communication Engineers of Japan.

Masatoshi Nakayama was born in Nagano, Japan, on November 2, 1963. He received the B.Sc. and M.Sc. degrees in astronomy in 1986 and 1988, respectively and the D.E. degree in electronic engineering in 1991 from Tohoku University, Sendai, Japan.

In 1991, he joined Mitsubishi Electric Corporation, Kanagawa, Japan.

Mr. Nakayama a member of the Institute of Electronics, Information and Communication Engineers of Japan.

Katsumi Osakabe was born in Tokyo, Japan, on February 27, 1968. He received the B.E. degree in electronic engineering from Tohoku University, Sendai, Japan, in 1991.

In 1991 he joined Mitsubishi Bank.

Toshihide Tanaka was born in Osaka, Japan, on October 8, 1965. He received the B.E. and M.E. degrees in electronic engineering from Tohoku University, Sendai, Japan, in 1989 and 1991, respectively.

In 1991 he joined The Chubu Electric Power Co., Inc., Japan.

Koji Mizuno (M'72–SM'72), for a photograph and biography, see this issue, p. 811.